Proteomic characterization of cytoskeletal and mitochondrial class III β-tubulin

Lucia Cicchillitti,[1] Roberta Penci,[1] Michela Di Michele,[2] Flavia Filippetti,[1] Domenico Rotilio,[2] Maria Benedetta Donati,[2] Giovanni Scambia,[1] and Cristiano Ferlini[1]

[1]Department of Oncology and [2]Research Laboratories, Catholic University of the Sacred Heart, Campobasso, Italy

Abstract

Class III β-tubulin (TUBB3) has been discovered as a marker of drug resistance in human cancer. To get insights into the mechanisms by which this protein is involved in drug resistance, we analyzed TUBB3 in a panel of drug-sensitive and drug-resistant cell lines. We identified two main different isoforms of TUBB3 having a specific electrophoretic profile. We showed that the apparently higher molecular weight isoform is glycosylated and phosphorylated and it is localized in the cytoskeleton. The apparently lower molecular weight isoform is instead found exclusively in mitochondria. We observed that levels of phosphorylation and glycosylation of TUBB3 are associated with the resistant phenotype and compartmentalization into cytoskeleton. By two-dimensional nonreduced/reduced SDS-PAGE analysis, we also found that TUBB3 protein *in vivo* forms protein complexes through intermolecular disulfide bridges. Through TUBB3 immunoprecipitation, we isolated protein species able to interact with TUBB3. Following trypsin digestion, these proteins were characterized by mass spectrometry analysis. Functional analysis revealed that these proteins are involved in adaptation to oxidative stress and glucose deprivation, thereby suggesting that TUBB3 is a survival factor able to directly contribute to drug resistance. Moreover, glycosylation of TUBB3 could represent an attractive pathway whose inhibition could hamper cytoskeletal compartmentalization and TUBB3 function. [Mol Cancer Ther 2008;7(7):2070–9]

Received 12/5/07; revised 3/3/08; accepted 3/4/08.

Grant support: Italian Ministry for University and Research.

The costs of publication of this article were defrayed in part by the payment of page charges. This article must therefore be hereby marked *advertisement* in accordance with 18 U.S.C. Section 1734 solely to indicate this fact.

Requests for reprints: Cristiano Ferlini, Department of Oncology, Catholic University of the Sacred Heart, Largo A. Gemelli, 1-86100, Campobasso, Italy. Phone: 39-08-74312477; Fax: 39-08-74312324.
E-mail: cferlini@rm.unicatt.it

doi:10.1158/1535-7163.MCT-07-2370

Introduction

β-Tubulin, together with α-tubulin, participates in the formation of microtubules, the integrity of which is essential for the segregation of chromosomes during cell division, maintenance of cell shape, and intracellular trafficking of macromolecules and organelles (1).

Vertebrate α- and β-tubulins are each encoded by a 9- to 8-member multigene family, respectively, that produces highly homologous and conserved gene products in which the sequences are highly divergent only in their last 10 to 15 amino acids (2). These carboxyl-terminal sequences have been used to assign β-tubulin gene products to at least seven distinct classes (3). Each of these classes defines a β-tubulin isotype that differs significantly from other isotypes within the same organism but differs very little from the same isotype in other vertebrate species.

Class I and II are the most abundant β-tubulin isotypes and are constitutively expressed, whereas class III β-tubulin (TUBB3) has been reported previously to as an isotype specific for neuronal tissues and testis (2). However, this original view seems now incorrect, because TUBB3 expression has recently been observed in other tissues and particularly in the mitochondrial membrane where it exerts an unknown function (4). Several reports indicate that an increase in the relative abundance of TUBB3 isoform destabilizes the microtubules and correlates with drug resistance (5–8).

The carboxyl-terminal regions of both α and β-tubulin undergo numerous posttranslational modifications capable to modulate the function of the microtubule, such as glutamylation, glycosylation, tyrosination, acetylation, and acylation (9, 10). Tubulin can also be phosphorylated by several kinases (11), and such changes affect the overall dynamic properties of cellular microtubules during interphase as well as mitosis (11–14). Khan and Luduena have also proposed that modification of certain cysteine residues of tubulin might regulate the dimer/microtubule equilibrium and that the thioredoxin system might, in turn, regulate this equilibrium (15).

TUBB3 has assumed an important role as a clinical marker of drug resistance in ovary (16), lung (17), stomach (18), pancreas (19), and breast (20) cancer patients. Due to the relevance clinically proven as a factor of drug resistance, here we report the results of a proteomic analysis of TUBB3 aimed to better characterize the protein function and possibly develop novel approaches to prevent or circumvent TUBB3-mediated drug resistance. Our data highlight that compartmentalization into mitochondrion and cytoskeleton is associated to a different pathway of posttranslational changes and that glycosylation and phosphorylation status of TUBB3 correlates with the paclitaxel-resistant phenotype. Moreover, TUBB3 appears

inserted in a functional network of factors involved in the adaptation to oxidative stress and glucose deprivation, thereby suggesting that it is a part of a survival pathway that directly contributes to the acquisition of the drug-resistant phenotype.

Materials and Methods

Antibodies and Drugs

Polyclonal anti-TUBB3 (PRB-435P) and monoclonal (SDL.3D10) were purchased from Covance and Sigma, respectively. Polyclonal antibody anti-tubulin (H-235) was obtained from Santa Cruz Biotechnology. Anti β-tubulin class I + II (T8535) monoclonal antibody, concanavalin A peroxidase labeled (L6396), wortmannin, and tunicamycin were purchased from Sigma. Validation of the antibodies has been done using the protocol described by Hiser et al. (21).

Cell Culture and Gel Electrophoresis

Cell culture procedures and cell line and growth inhibition experiments have been elsewhere described (22). Cells harvested in cold PBS were extracted for 30 min at 4°C in lysis buffer [50 mmol/L Tris-HCl (pH 7.4), 150 mmol/L NaCl, 1% NP-40] containing 1 mmol/L DTT, protease inhibitor cocktail (Roche), and phosphatase inhibitors (50 mmol/L NaF, 0.2 mmol/L Na_3VO_4). After centrifugation, supernatants (300 μg from total lysates and 100 μg from mitochondrial extracts) were immunoprecipitated at 4°C overnight in lysis buffer by adding Protein A/G Plus-agarose beads (Santa Cruz Biotechnology) after 2 h of incubation with 2 μg anti-TUBB3 polyclonal antibody. Western blots were done as described previously (22). Immunoblots were developed using SuperSignal West Femto chemiluminescent reagents (Pierce) according to the manufacturer's instructions.

For two-dimensional SDS-PAGE analysis, proteins were dissolved in the isoelectric focusing solution containing 8 mol/L urea, 4% CHAPS, and 2% carrier ampholyte (pH 3-10). The IPG strips (pH 3-10 nonlinear, 7 cm long; GE-Healthcare) were rehydrated with isoelectric focusing solution with 0.002% bromophenol blue containing protein sample to carry out analytical analysis in Ettan IPGphor II (GE-Healthcare) for 12 h at 20°C. The rehydrated strips were focused at 20°C using the following running conditions: 300 V for 4 h, voltage gradient from 300 to 1,000 V in 1 h, voltage gradient from 1,000 to 5,000 V in 2 h, and 5,000 V for 40 min. Before running the second dimension, the IPG strips were equilibrated for 15 min in equilibration buffer [6 mol/L urea, 2% (w/v) SDS, 50 mmol/L Tris-HCl (pH 8.8), 30% (v/v) glycerol] with 10 mg/mL DTT and for 15 min with equilibration buffer containing 25 mg/mL iodoacetamide. To study the possibility of TUBB3 carboxymethylation due to iodoacetamide, the last equilibration step was omitted. Electrophoresis in the second dimension was carried out in 10% polyacrylamide gels. The IPG strips were embedded with 0.5% (w/v) melted agarose solution before running on the SDS-PAGE slabs.

For two-dimensional nonreduced/reduced SDS-polyacrylamide gel, proteins were mixed in nonreducing SDS-PAGE sample buffer [0.25 mmol/L Tris-HCl (pH 6.8), 2% (w/v) SDS, 20% (v/v) glycerol, 0.004% (w/v) bromophenol blue] and separated by SDS-PAGE on a 10% acrylamide gel. Gel lanes were excised and incubated in buffer containing 50 mmol/L DTT for 10 min and further 10 min in 100 mmol/L iodoacetamide before separation through a second SDS-PAGE gel (10%). Proteins were visualized by silver staining. Chromatography analysis was done using the Q-proteome glycoprotein kit and the phosphoprotein purification kit purchased from Qiagen.

RNA Extraction and Real-time PCR

Total cellular RNA was obtained from cells A2780 and TC1 by using BioRobot EZ1 according to the manufacturer's directions (Qiagen). The TUBB3 gene is organized into four exons and four introns. Using real-time PCR analysis, we evaluated the possibility of isoforms in gene transcript due to events of alternative splicing.

RNA (1 μg) was reverse transcribed into cDNA using the iScript cDNA Synthesis Kit (Bio-Rad). PCR was done in a final volume of 25 μL using the iQ SYBR Green Supermix (Bio-Rad) with 10 μmol/L primers designed using the Beacon Designer 3 Software (Premier Biosoft International). We used primer combination amplifying overlapping fragments corresponding to entire TUBB3 coding sequence (TUBB3 forward 5′-ATGAGGGAGATCGTGCAC-3′ and TUBB3 reverse 5′-TCCAGGACCGAATCCACCA-3′) and to region lacking of exon 2 (B3 splicing 2 forward 5′-GATCGGGGCCAAGCTCACAAG-3′ and TUBB3 reverse 5′-TCCAGGACCGAATCCACCA-3′) or exon 3 (B3 splicing forward 5′-TACTACAACGAGGCCTCTTGTCAG-3′ and TUBB3 reverse 5′-TCCAGGACCGAATCCACCA-3′).

PCR amplifications were done using an Opticon 2 System (Bio-Rad) starting with a 3-min template denaturation step at 95°C followed by 40 cycles of 15 s at 95°C and 45 s at 56.7°C (for the entire TUBB3 and for the region lacking exon 3) or 63.5°C (for the region lacking exon 2). The amplification products were analyzed on 2.0% agarose gels, stained with ethidium bromide, visualized under UV light, and photographed.

Mitochondria and Cytoskeletal Fraction Isolation

Mitochondria isolation was done as described previously (23). Microtubules proteins were isolated from cell lines by three cycles of polymerization and depolymerization. Briefly, cell pellets were homogenated in PB buffer [0.1 mol/L K-PIPES (pH 6.8), 0.5 mmol/L $MgCl_2$, 2 mmol/L EGTA, 0.1 mmol/L EDTA, 0.1% β-mercaptoethanol, 1 mmol/L ATP, protease and phosphatase inhibitors] and centrifuged at 100,000 × *g* for 60 min at 4°C. Cytosolic supernatants were collected and mixed with half volume of 100% glycerol preheated at 37°C and GTP, ATP, and $MgCl_2$ were added at the concentrations of 0.1, 1, and 3.5 mmol/L, respectively, and incubated at 37°C for 60 min to polymerize. After centrifugation at 100,000 × *g* for 45 min at 37°C, pellets were collected, resuspended with ice-cold PB buffer, and incubated on ice for 30 min to depolymerize. This process was repeated twice.

Tubulin Polymerization Assay

Cells were washed twice with PBS and lysed for 5 min with 100 μL hypotonic buffer [1 mmol/L $MgCl_2$, 2 mmol/L EGTA, 0.5% NP40, protease and phosphatase inhibitors, 20 mmol/L Tris-HCl (pH 6.8)]. The samples were centrifuged at 14,000 rpm for 10 min at room temperature, and the supernatants containing soluble tubulin were separated from the pellets containing assembled tubulin. Each fraction was mixed with 5× SDS-PAGE sample buffer, heated for 10 min at 95°C, and analyzed by SDS-PAGE.

Mass Spectrometry and Protein Identification

Spots and bands of interest were manually excised from polyacrylamide gels and sliced into small pieces. The gel pieces were destained by washing twice with 6 mmol/L potassium ferricyanide in 100 g/L sodium thiosulfate and dehydrated with acetonitrile. Next, the pieces were dried in a vacuum centrifuge and digested overnight with 5 μL of 20 ng/μL trypsin (Sigma) in 40 mmol/L ammonium bicarbonate/10% acetonitrile at 37°C. The digestion reaction was blocked by adding 10 μL of 1% trifluoroacetic acid. The proteolytic peptides were extracted with 50% acetonitrile/0.1% trifluoroacetic acid, dried in a vacuum centrifuge, and reconstituted in 5 μL of 50% acetonitrile/0.1% trifluoroacetic acid. The sample solution (0.5 μL) was mixed with 0.5 μL α-cyano-4-hydroxycinnamic acid (10 mg/mL in 50% acetonitrile/0.1% trifluoroacetic acid) and spotted onto a matrix-assisted laser desorption/ionization target.

Peptide mass fingerprinting was done on a Voyager-DE STR matrix-assisted laser desorption/ionization time-of-flight mass spectrometer (Applied Biosystems), operating in positive ion reflectron mode, with an acceleration voltage of 20 kV. Spectra were analyzed using the DataExplorer software v4.0 (Applied Biosystems). All mass spectra were calibrated with a calibration kit (Applied Biosystems). Mascot software (Matrix Science) was employed for protein database searching using monoisotopic mass values for each spectrum. The searches were done using the National Center for Biotechnology Information and SWISS-PROT databases and the following standard variables: *Homo sapiens*; tryptic digest with a maximum number of one missed cleavage; carboxyamidomethylation of cysteine, and partial methionine oxidation. Identifications were accepted based on a tripartite evaluation that takes in account significant MOWSE score,

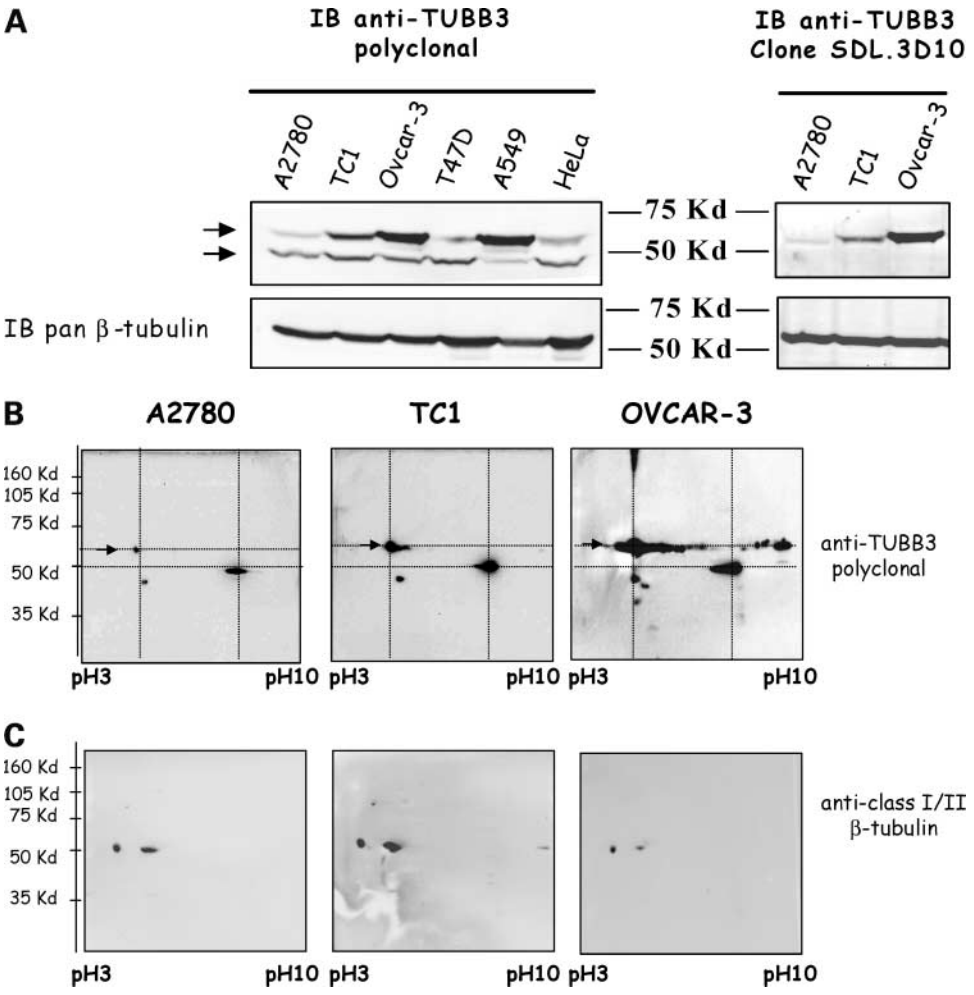

Figure 1. TUBB3 electrophoretic profile is characterized by two main forms: a faster migrating band and a slow migrating band. **A**, immunoblot with anti-TUBB3 polyclonal and monoclonal antibodies showing that the two TUBB3 isoforms are visible in various cell lines only with the polyclonal anti-TUBB3. **B**, two-dimensional SDS-PAGE analysis revealed that the faster migrating form of TUBB3 has a more basic p*I*. This is a peculiar characteristic of TUBB3, because isotype I and II β-tubulins migrate at the expected p*I* (**C**).

spectrum annotation, and observed versus expected migration on two-dimensional gel. The MASCOT MOWSE score is defined as $-10 * \log P$, where P is the probability that the observed match is a random event. A score of 64 corresponds to $P < 0.05$ for our data set and was chosen as the cutoff for a significant hit.

Results

Electrophoretic Profile and Localization of TUBB3 Isoforms

TUBB3 levels were analyzed in a panel of human cancer cell lines coming from several human cancer tissues. A2780 cells are drug-sensitive human ovarian cancer cells, whereas TC1 cell line is its counterpart made drug resistant to paclitaxel. OVCAR-3 cells are another human ovarian cancer cell line with a profile of native drug resistance. T47D, A549, and HeLa cells are human cancer cell lines coming from breast, lung and cervix, respectively. The profile of chemosensitivity of the most commonly used chemotherapeutics is reported in Supplemental Data.[3]

Due to the presence of a wide overlap in the sequences, at the beginning, we validated with a specific protocol adapted from Hiser et al. (21) the use of two specific anti-TUBB3 antibodies (mouse monoclonal SDL.3D10 and rabbit polyclonal PRB-435P) raised against the same immunogen at the carboxyl terminus of the protein. Both antibodies were able to interact selectively only with TUBB3 and not with the other β-tubulin isotypes (Supplementary Fig. S1). However, when used in a panel of cells, the polyclonal PRB-435P antibody reacted with two main TUBB3 isoforms in one-dimensional Western blot, whereas the monoclonal SDL.3D10 identified only the fastest migrating band (Fig. 1A). When comparing TUBB3 expression in drug-sensitive versus drug-resistant cells with the polyclonal antibody, the lowest TUBB3 isoform was not modulated, whereas the highest one appears overexpressed in drug-resistant cells, in that confirming previous results obtained in paclitaxel-resistant cells (22).

Due to the superior discriminating properties of the polyclonal antibody, we decided to use throughout this study the polyclonal antibody. As a second approach, we analyzed the migration pattern of TUBB3 from ovarian cancer cells on two-dimensional gels. The faster migrating form of TUBB3 has a more basic isoelectric point (pI = 7.0) than the expected (pI = 4.8; Fig. 1B). Moreover, we observed that this is a peculiar characteristic of TUBB3, because class I and II β-tubulin migrate at the expected isoelectric point (Fig. 1C). To correlate the two isoforms with an intracellular distribution pattern, mitochondrial and cytoskeletal fractions were separated and two-dimensional gel analysis was repeated in the three cell lines. The lower band was detectable only in the mitochondrial compartment (Fig. 2A), whereas the upper band was present in both cytoskeletal and mitochondrial preparations (Fig. 2A). To further characterize TUBB3 compartmentalization, we separated polymerized and free tubulin fractions through ultracentrifugation and we repeated Western blot for TUBB3. Also, in this case, only the upper band of TUBB3 was found in the polymerized fraction, thereby confirming that it represents cytoskeletal TUBB3 (Fig. 2B).

TUBB3 Isoforms Are Not Generated by Alternative Splicing

The TUBB3 gene is organized into four exons and three introns. Using real-time PCR analysis, we evaluated the possibility of isoforms in gene transcript due to events of alternative splicing. We used primer combination amplifying overlapping fragments corresponding to entire TUBB3 coding sequence and to region lacking of exon 2 or 3. The amplification products were analyzed on 2% agarose gels, stained with ethidium bromide, visualized under UV light, and photographed.

This approach did not provide evidence of TUBB3 mRNA isoforms able to explain the generation of the two isoforms (Supplementary Fig. S2).[3] Therefore, this finding prompted us to investigate posttranslational changes as responsible for the generation of the two isoforms of TUBB3.

Identification of the Pathways Involved in Posttranslational Changes of TUBB3

To understand if the level of TUBB3 glycosylation and/or phosphorylation has a role in its localization and function, we treated A2780, TC1, and OVCAR-3 cells with inhibitors of glycosylation (tunicamycin) and phosphoinositide 3-kinase (PI3K)–dependent phosphorylation (wortmannin). Exposing cells to tunicamycin disrupts glycosylation of newly synthesized proteins. This is due to the blockage of the transference of the 14-residue core oligosaccharide (containing two *N*-acetylglucosamine, nine mannose, and three glucose residues) from a dolichol phosphate donor molecule to certain asparagine residues on the proteins. Wortmannin, a metabolite of the fungus *Penicillium funiculosum*, is a specific inhibitor of PI3K. Blockade of the PI3K-Akt pathway induces the activation of glycogen synthase kinase-3β, which phosphorylates microtubule-associated proteins and thereby modulates their ability to bind and stabilize microtubules. The PI3K pathway is one of the major signaling pathways regulating cellular growth and transformation and it has been found associated to microtubules (24). We treated the cells for 8 h with sublethal doses of drugs. A shift toward a more basic pI of cytoskeletal TUBB3 was noticed using both inhibitors in total lysates (Fig. 3). Along with the shift, it was evident in one-dimensional Western blot a reduction in the intensity of the signals in OVCAR-3 cells, so indicating a reduction in cytoskeletal compartmentalization (data not shown). On the other hand, in mitochondria, we were not able to detect any shift, in that suggesting that glycosylation and phosphorylation are not involved in mitochondrial localization. These findings suggest that TUBB3 is a downstream substrate of the PI3K pathway and that glycosylation and

[3] Supplementary material for this article is available at Molecular Cancer Therapeutics Online (http://mct.aacrjournals.org/).

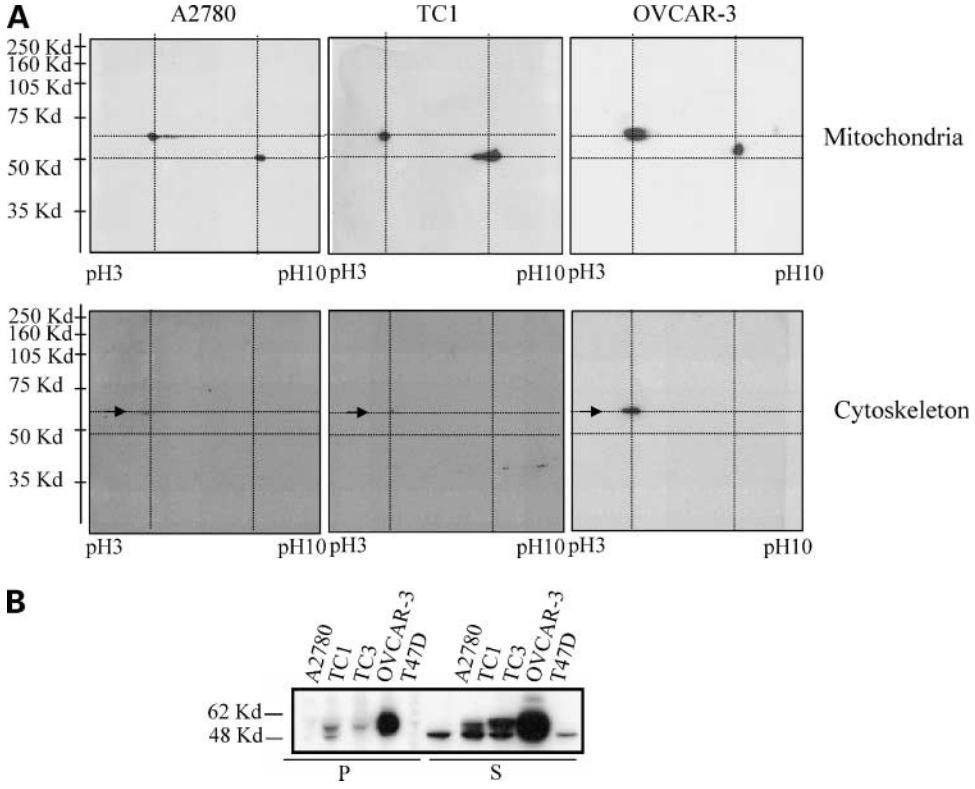

Figure 2. The two TUBB3 isoforms have a specific cellular distribution. **A**, the slower migrating TUBB3 form is localized in both mitochondria and cytoskeleton, whereas the faster migrating one is detected only in the mitochondrial compartment. **B**, tubulin polymerization assay showing that the slower migrating TUBB3 form is mainly associated with the pellet containing assembled tubulin (*P*), whereas the faster migrating form is instead exclusively localized in the soluble fraction of tubulin (*S*).

phosphorylation act in concert to direct TUBB3 into cytoskeleton. However, due to the broad activity of wortmannin, we cannot exclude that additional kinases diverse from PI3K could mediate TUBB3 phosphorylation.

TUBB3 Is Glycosylated and Phosphorylated

To get further insights into posttranslational changes of TUBB3, we did chromatography affinity studies using total lysates from A2780, TC1, and OVCAR-3 cells. As a first approach, the presence of phosphorylation was assessed through immunoprecipitation with phosphothreonine and phosphoserine antibodies (Fig. 4A). The upper band of TUBB3 resulted phosphorylated, whereas no phosphorylation pattern was detectable in the lower band, which was collected in the flow-through fraction. On the other hand, class I and II β-tubulin was completely phosphorylated. This finding suggests again that phosphorylation is a prerequisite for cytoskeletal localization.

To assess the presence of glycosylation, in the same cell lysates glycoproteins were separated using affinity chromatography for concanavalin A and wheat germ agglutinin lectins. Concanavalin A recognizes α-linked mannose and terminal glucose residues, whereas wheat germ agglutinin lectin selectively binds to *N*-acetylglucosamine groups and to sialic acid. Results show that the upper band of TUBB3 is glycosylated and recognized by both lectins, whereas class I and II β-tubulin are not glycosylated. The levels of glycosylation and phosphorylation of TUBB3 were higher in the TC1 and OVCAR-3 drug-resistant cells compared with that noticed in drug-sensitive A2780 cells (Fig. 4A), thereby suggesting that these posttranslational modifications are associated with cytoskeletal distribution and acquisition of the resistant phenotype. In keeping with this view, the eluted fractions containing phosphoproteins and glycoproteins were then run again in two-dimensional gel electrophoresis and immunoblot revealed that TUBB3 migrate in correspondence to the cytoskeletal pattern above described (pH 4.8 and upper band; Fig. 4B).

Identification of TUBB3 Complexes

Identification of the protein species able to interact with TUBB3 could provide important information on the mechanisms through which this protein is involved in drug resistance. A critical issue in proteomic studies is the reproducibility and all the experiments were done in triplicates and the protein species were considered if identified in all the three independent experiments. We did immunoprecipitation experiments with anti-TUBB3 antibody using total lysates and mitochondrial extracts from A2780, TC1, and OVCAR-3 cells. To identify proteins forming mixed disulfide bonds with TUBB3, eluted proteins from immunoprecipitation were subjected to two-dimensional nonreduced/reduced SDS-PAGE analysis with first dimension carried out under nonreducing conditions to separate mixed disulfide complexes and the second dimension run on reducing conditions to resolve the mixed disulfides according to their individual size (25).

Immunodetection using anti-TUBB3 antibody after two-dimensional nonreduced/reduced SDS-PAGE PAGE

analysis confirmed that the cysteine residues in TUBB3 protein form intermolecular disulfide bridges because some complexes migrate below the diagonal. Immunodetection using anti-TUBB3 antibody after two-dimensional nonreduced/reduced SDS-PAGE analysis confirmed that the cysteine residues in TUBB3 protein form intermolecular disulfide bridges because a smear, corresponding to oligomer forms, migrating below the diagonal, was detected. In particular, these complexes were detectable in OVCAR-3 cells where TUBB3 is highly expressed (Fig. 5). To identify the complexes, the protein species migrating below the diagonal were excised from the gel and identified by matrix-assisted laser desorption/ionization time-of-flight mass spectrometry. Detected proteins are reported in Table 1. One major complex associated to TUBB3 is composed by vimentin/dimethylalanine monooxygenase 4 [*N*-oxide-forming] (FMO4) and another one involves glutathione transferase M4. In parallel, complexes present in the diagonal not linked to interactions via disulfide bridge were excised and analyzed. Several cytoskeletal elements were detected, such as β-actin, tropomyosin 3, and GRP78. Unexpectedly, it was also found associated to TUBB3 nucleolin, a protein involved in the control of transcription of rRNA genes by RNA polymerase I, in ribosome maturation and assembly, and in nucleocytoplasmic transportation of ribosomal components (26).

To gain insight into the interactions present at the mitochondrial level, we did immunoprecipitation experiments with anti-TUBB3 antibody using mitochondrial extracts from A2780, TC1, and OVCAR-3 cells. Resolved bands detected in all cell types studied were excised from the gel and proteins were identified by matrix-assisted laser desorption/ionization time-of-flight mass spectrometry in all the three experiments were considered (Table 1). Mitochondrial preparations are always associated to microtubules. For this fact, some proteins isolated after immunoprecipitation from mitochondria belong again to the cytoskeletal fraction, such as β-actin, vimentin, and tropomyosin 3. Additional proteins reported as cytoskeletal were TUBA1B, GRP75, CDC14A, IVL, keratin 9, and keratin 10. TUBB3 was associated also with PKM2, a glycolytic enzyme that catalyzes the transfer of a phosphoryl group from phosphoenolpyruvate to ADP, generating ATP. Interactions were found also for GABBR1, a receptor for γ-aminobutyric acid, involucrin, and an unknown protein kinase similar to casein kinase 1. Taken together, all these interactions, it seems evident that TUBB3 is intimately bound to a series of proteins involved in the response to oxidative stress and glucose deprivation.

Discussion

Among the factors related to drug resistance, TUBB3 plays a prominent role in several tissues. Recently, Gan et al. (27) have shown that TUBB3 is overexpressed not only in cells treated with microtubule-interacting agents, such as taxanes and *Vinca* alkaloids, but also in cells resistant to DNA-damaging drugs such as cisplatin. Therefore, this finding suggests that TUBB3 represents an important factor of resistance and a main component of a survival program alas activated in drug-resistant patients.

This work was mainly aimed to identify a novel druggable pathway useful to block TUBB3 function in drug-resistant cells. So, we discovered that two TUBB3 isoforms exist in the cells. The first one is localized in the mitochondrion, is unglycosylated and unphosphorylated, and is not overexpressed in drug-resistant cells. During gel electrophoresis, mitochondrial TUBB3 exhibits a basic shift

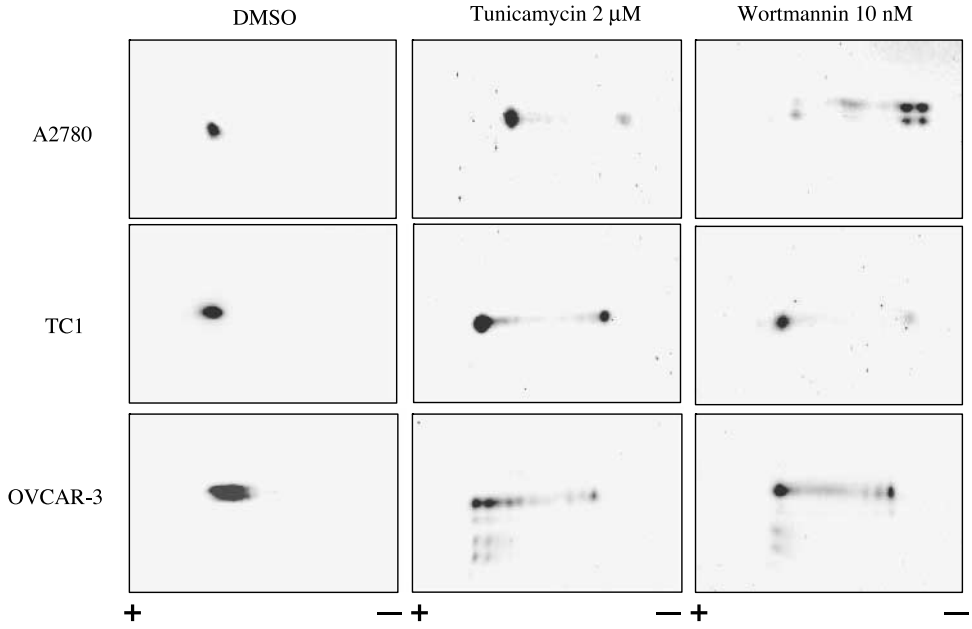

Figure 3. Cells were treated for 8 h with sublethal doses of tunicamycin (2 μmol/L) or wortmannin (10 nmol/L) and cellular lysates subjected to two-dimensional SDS analysis. Total lysates from A2780 and from TC1 and OVCAR-3 cells treated and not treated with tunicamycin or wortmannin were separated on two-dimensional SDS-PAGE. Immunoblot with anti-TUBB3 polyclonal antibody showed a decrease in the intensity of the signal and a shift toward a more basic p*I*.

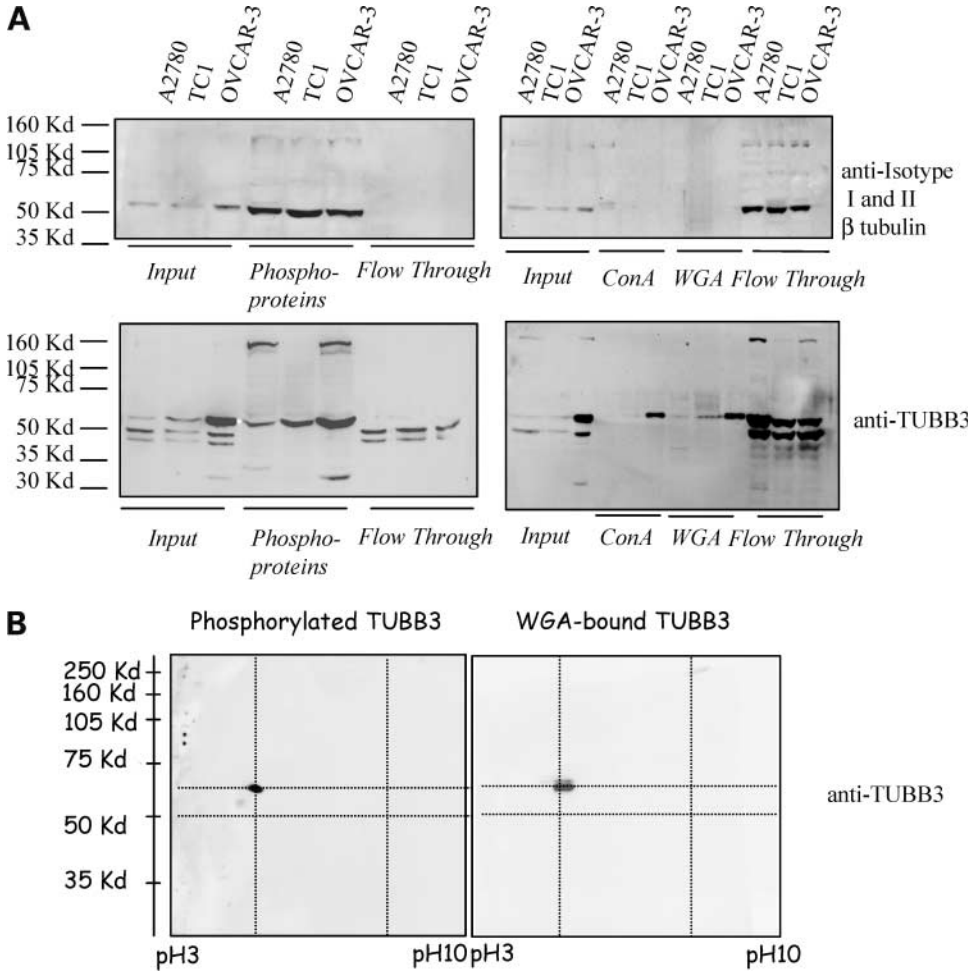

Figure 4. The slow migrating TUBB3 corresponds to a glycosylated and phosphorylated form. **A,** immunoblot with concanavalin A peroxidase labeled or anti-TUBB3 after immunoprecipitation with anti-TUBB3 polyclonal antibody of total and mitochondrial lysates from A2780, TC1, and OVCAR-3 cells. **B,** immunoblot with anti-TUBB3 polyclonal antibody and anti class I and II β-tubulin antibody after separation from total lysates of phosphorylated and unphosphorylated proteins through affinity chromatography and of glycosylated and unglycosylated proteins using wheat germ agglutinin affinity column.

in the isoelectric point and a higher mobility, conferring to the isoform an apparently lower molecular weight. This pattern in principle could be dependent on (*a*) a genetic isoform, (*b*) a protein cleavage, and (*c*) a posttranslational change. For that concerning (*a*), we have directly excluded this hypothesis, because primers designed to identify splicing variants failed to detect genetic isoforms. The hypothesis (*b*) could be supported by a report where it was shown that α-tubulin is a substrate for the cytosolic serine protease granzyme B and that the truncated product is not associated with polymerized microtubules (28). However, it seems unlikely that the mitochondrial TUBB3 isoform is due to a carboxyl-terminal cleavage, because it is still recognized by the antibody raised against the last residues of the carboxyl-terminal domain. Moreover, because the most acidic part of TUBB3 is located at the carboxyl terminus, it is also improbable that a cleavage at the amino terminus occurs. This makes more possible that the difference in the gel mobility is dependent on (*c*). According to previous reports (29, 30), the involved posttranslational change could be an alkylation, which is, to our knowledge, the only change that produces a difference in the net charge of the protein capable to underlie a basic shift in the p*I* of this order and the concomitant faster migration during gel electrophoresis.

The second TUBB3 isoform is phosphorylated and glycosylated and compartmentalized into the cytoskeleton. It represents the isoform modulated in drug-resistant cells. We used tunicamycin and wortmannin to inhibit glycosylation and PI3K-dependent phosphorylation, respectively. Our results showed that both pathways are involved because a reduction in the cytoskeletal expression of the protein was obtained on exposure of cells to both agents, thereby showing that TUBB3 glycosylation and phosphorylation direct TUBB3 to cytoskeleton. This finding makes this pathway a potential target for development of novel drugs. In particular, glycosylation seems attractive, because this posttranslational change is specific of TUBB3 and not shared by the most commonly expressed class I and II isotype.

TUBB3 has plenty of interacting surfaces and interacts with a plethora of accessory proteins, whose function needs still to be characterized and which contribute to its intracellular distribution. This analysis allowed us to

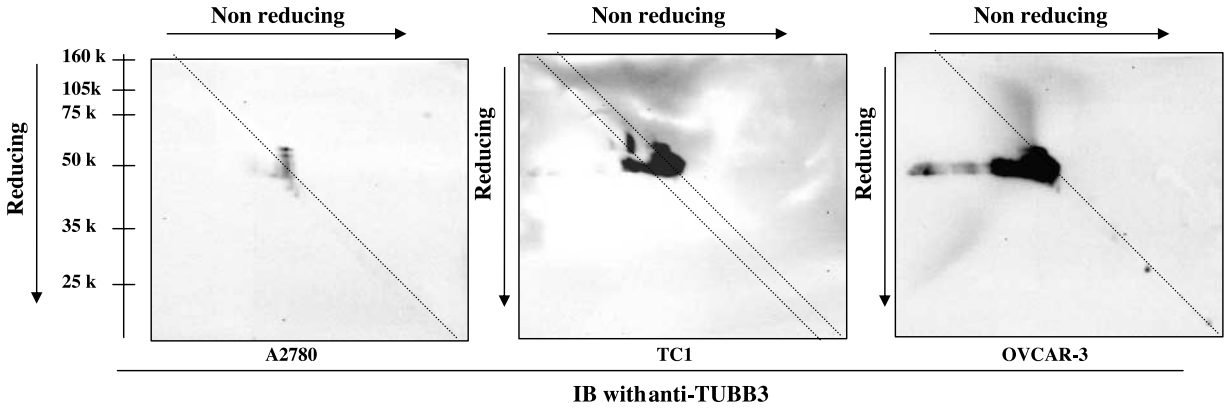

Figure 5. Immunoblotting with anti-TUBB3 antibody after two-dimensional nonreduced/reduced SDS-PAGE. Proteins lacking disulfide bonds will migrate on the diagonal (*gray line*) because of the identical mobility in both dimensions. Proteins that contain intrachain disulfide bonds will be more compact and will run above the diagonal; proteins that form interchain disulfide-linked complexes will run below the diagonal. *Arrows,* two major TUBB3 disulfide complexes picked and identified with mass spectrometry.

identify HSP70/GRP75 among the protein associated to TUBB3. This finding supports that GRP78/GRP75 and HSP/HSC70 play the cooperative role of molecular chaperones in formation and function of the eukaryotic cell cytoskeleton (31). Interestingly, we also found that FMO4 forms a complex mediated by disulfide bridges with TUBB3. FMO4 belongs to the flavin-containing monooxygenase family of enzymes able to oxidize drugs and xenobiotics containing a ''soft nucleophile,'' usually nitrogen or sulfur. Previous articles showed that FMO4 is

Table 1. Proteins which interact with TUBB3 in A2780, TC1, and OVCAR-3 cell lines

Identification	Gene name	Accession	MWth	p*I*th	Score	Matches	Coverage (%)
Total lysates							
Actin, β	ACTB	AAH12854	40,536	5.55	74	8	30
BiP protein	GRP78	AAF13605	71,002	5.23	94	23	42
Dihydrolipolylysine residue succinyltransferase component of 2—oxoglutarate dehydrogenase complex, mitochondrial (precursor)	DLST	P36957	48,640	9.01	84	8	19
Dimethylaniline monooxygenase 4 [*N*—oxide forming]*	FMO4	P31512	63,343	8.75	71	6	14
Glutathione transferase μ4*	GSTM4	Q03013	25,561	6.24	46	3	14
Nucleolin	NCL	P19338	76,614	4.59	79	9	18
Tropomyosin 3	TPM3	Q5VU72	28,890	4.76	70	6	28
Vimentin*	VIM	P08670	53,676	5.06	102	16	44
Mitochondria							
Actin, β	NA	Q96HG5	41,321	5.56	79	9	36
Cell division cycle 14 A	CDC14A	Q5VUH7	44,450	8.73	85	11	42
γ-Aminobutyric acid receptor B receptor, 1	GABBR1	Q5STL4	100,918	8.44	79	9	36
Heat shock 70-kDa protein 9 precursor	GRP75	P38646	73,680	5.87	85	12	25
Heat shock 70-kDa protein 9B variant	NA	Q53H23	73,874	5.87	80	9	20
Involucrin	IVL	P07476	68,468	4.62	65	7	19
Keratin 10	KRT10	P13645	59,020	5.09	72	12	24
Keratin 9, type I, cytoskeletal	KRT9	P35527	62,178	5.14	68	9	35
Pyruvate kinase isozymes M1/M2	PKM2	P14618	58,339	7.95	124	20	41
Similar to casein kinase 1	NA	CAC88317	53,072	9.13	71	8	29
Tubulin α-1 chain	TUBA1B	P68363	50,804	4.94	133	16	45
Vimentin	VIM	P08670	53,676	5.06	214	22	54

NOTE: Proteins from total lysates and mitochondrial extracts were immunoprecipitated with anti—TUBB3 antibody and separated by two-dimensional SDS–PAGE or two-dimensional nonreduced/reduced SDS–PAGE and identified by peptide mass fingerprinting with matrix-assisted laser desorption/ionization time-of-flight MS. The data include protein name, gene name (NA, not available), accession number in National Center for Biotechnology Information database, theoretical molecular mass (Mrth) and isoelectric point (p*I*th), MASCOT score, number of matching peptides, and percentage of sequence coverage by matching peptides.

*Proteins that formed mixed disulfides with TUBB3.

involved in the control of cellular redox state and in disulfide bond formation during protein synthesis and to regulate thiol/disulfide ratios in the cell (32). It has been already shown that cysteine residues in tubulin are actively involved in regulating ligand interactions and microtubule formation both *in vivo* and *in vitro* and that disulfides assist in correct refolding of tubulin from the intermediate unfolded state or help to recover the hydrophobic domains from the completely unfolded state (33). Moreover, associated to TUBB3, we identified the pyruvate kinase, a glycolytic kinase already found to play a role as glycolytic control enzyme as well as a microtubule destabilizer into the cytoskeleton (34). From a functional analysis of the network of proteins associated to TUBB3, it appears clear that many of them are involved in oxidative stress and glucose deprivation response. This finding suggests that TUBB3 is functionally involved in a survival pathway able to adapt cells to a microenvironment featured by low oxygen levels and poor nutrient supply. This function is enhanced in drug-resistant cells, thereby providing them the ability to survive the solid tumor microenvironment of the most aggressive diseases. This finding complements our recent discovery that TUBB3 is a factor activated by hypoxia and under the transcriptional control of HIF-1α (35).

In summary, here we show that at least two major isoforms of TUBB3 are obtained inside the cells through specific posttranslational changes and that through this mechanism TUBB3 acquires a specific pattern of intracellular distribution. This discovery could help in the discrimination of the protein function, thus providing a novel tool to better employ this protein as a marker of drug resistance separating the equally expressed mitochondrial isoform from the cytoskeletal one, which is up-regulated in drug-resistant cells. Moreover, the identification of the posttranslational changes involved in cytoskeletal localization could represent a novel druggable target which could be useful in the fight against drug resistance.

Disclosure of Potential Conflicts of Interest

No potential conflicts of interest were disclosed.

Acknowledgments

We thank Cristiana Gaggini and Federica Pignatelli for the expert technical assistance.

References

1. Dutcher SK. Motile organelles: the importance of specific tubulin isoforms. Curr Biol 2001;11:R419 – 22.

2. Cleveland DW, Sullivan KF. Molecular biology and genetics of tubulin. Annu Rev Biochem 1985;54:331 – 65.

3. Lopata MA, Cleveland DW. *In vivo* microtubules are copolymers of available β-tubulin isotypes: localization of each of six vertebrate β-tubulin isotypes using polyclonal antibodies elicited by synthetic peptide antigens. J Cell Biol 1987;105:1707 – 20.

4. Carre M, Andre N, Carles G, et al. Tubulin is an inherent component of mitochondrial membranes that interacts with the voltage-dependent anion channel. J Biol Chem 2002;277:33664 – 9.

5. Panda D, Miller HP, Banerjee A, Luduena RF, Wilson L. Microtubule dynamics *in vitro* are regulated by the tubulin isotype composition. Proc Natl Acad Sci U S A 1994;91:11358 – 62.

6. Derry WB, Wilson L, Khan IA, Luduena RF, Jordan MA. Taxol differentially modulates the dynamics of microtubules assembled from unfractionated and purified β-tubulin isotypes. Biochemistry 1997;36: 3554 – 62.

7. Verdier-Pinard P, Wang F, Martello L, et al. Analysis of tubulin isotypes and mutations from taxol-resistant cells by combined isoelectrofocusing and mass spectrometry. Biochemistry 2003;42:5349 – 57.

8. Kamath K, Wilson L, Cabral F, Jordan MA. βIII-tubulin induces paclitaxel resistance in association with reduced effects on microtubule dynamic instability. J Biol Chem 2005;280:12902 – 7.

9. MacRae TH. Tubulin post-translational modifications—enzymes and their mechanisms of action. Eur J Biochem 1997;244:265 – 78.

10. Westermann S, Weber K. Post-translational modifications regulate microtubule function. Nat Rev Mol Cell Biol 2003;4:938 – 47.

11. Verde F, Labbe JC, Doree M, Karsenti E. Regulation of microtubule dynamics by cdc2 protein kinase in cell-free extracts of *Xenopus* eggs. Nature 1990;343:233 – 8.

12. Margolis RU, Margolis RK, Atherton DM. Carbohydrate-peptide linkages in glycoproteins and mucopolysaccharides from brain. J Neurochem 1972;19:2317 – 24.

13. Schaar BT, Kinoshita K, McConnell SK. Doublecortin microtubule affinity is regulated by a balance of kinase and phosphatase activity at the leading edge of migrating neurons. Neuron 2004;41:203 – 13.

14. Trinczek B, Brajenovic M, Ebneth A, Drewes G. MARK4 is a novel microtubule-associated proteins/microtubule affinity-regulating kinase that binds to the cellular microtubule network and to centrosomes. J Biol Chem 2004;279:5915 – 23.

15. Khan IA, Luduena RF. Possible regulation of the *in vitro* assembly of bovine brain tubulin by the bovine thioredoxin system. Biochim Biophys Acta 1991;1076:289 – 97.

16. Ferrandina G, Zannoni GF, Martinelli E, et al. Class III β-tubulin overexpression is a marker of poor clinical outcome in advanced ovarian cancer patients. Clin Cancer Res 2006;12:2774 – 9.

17. Seve P, Isaac S, Tredan O, et al. Expression of class III β-tubulin is predictive of patient outcome in patients with non-small cell lung cancer receiving vinorelbine-based chemotherapy. Clin Cancer Res 2005;11: 5481 – 6.

18. Urano N, Fujiwara Y, Doki Y, et al. Clinical significance of class III β-tubulin expression and its predictive value for resistance to docetaxel-based chemotherapy in gastric cancer. Int J Oncol 2006; 28:375 – 81.

19. Lee KM, Cao D, Itami A, et al. Class III β-tubulin, a marker of resistance to paclitaxel, is overexpressed in pancreatic ductal adenocarcinoma and intraepithelial neoplasia. Histopathology 2007;57:539 – 46.

20. Paradiso A, Mangia A, Chiriatti A, et al. Biomarkers predictive for clinical efficacy of taxol-based chemotherapy in advanced breast cancer. Ann Oncol 2005;16 Suppl 4:iv14 – 9.

21. Hiser L, Aggarwal A, Young R, et al. Comparison of β-tubulin mRNA and protein levels in 12 human cancer cell lines. Cell Motil Cytoskeleton 2006;63:41 – 52.

22. Mozzetti S, Ferlini C, Concolino P, et al. Class III β-tubulin overexpression is a prominent mechanism of paclitaxel resistance in ovarian cancer patients. Clin Cancer Res 2005;11:298 – 305.

23. Ferlini C, Raspaglio G, Mozzetti S, et al. Bcl-2 down-regulation is a novel mechanism of paclitaxel resistance. Mol Pharmacol 2003;64: 51 – 8.

24. Kapeller R, Chakrabarti R, Cantley L, Fay F, Corvera S. Internalization of activated platelet-derived growth factor receptor-phosphatidylinositol-3′ kinase complexes: potential interactions with the microtubule cytoskeleton. Mol Cell Biol 1993;13:6052 – 63.

25. Jessop CE, Chakravarthi S, Garbi N, et al. ERp57 is essential for efficient folding of glycoproteins sharing common structural domains. EMBO J 2007;26:28 – 40.

26. Srivastava M, McBride OW, Fleming PJ, Pollard HB, Burns AL. Genomic organization and chromosomal localization of the human nucleolin gene. J Biol Chem 1990;265:14922 – 31.

27. Gan PP, Pasquier E, Kavallaris M. Class III β-tubulin mediates sensitivity to chemotherapeutic drugs in non small cell lung cancer. Cancer Res 2007;67:9356 – 63.

28. Goping IS, Sawchuk T, Underhill DA, Bleackley RC. Identification of α-tubulin as a granzyme B substrate during CTL-mediated apoptosis. J Cell Sci 2006;119:858 – 65.

29. Legault J, Gaulin JF, Mounetou E, et al. Microtubule disruption induced *in vivo* by alkylation of β-tubulin by 1-aryl-3-(2-chloroethyl)ureas, a novel class of soft alkylating agents. Cancer Res 2000;60:985 – 92.

30. Bouchon B, Chambon C, Mounetou E, et al. Alkylation of β-tubulin on Glu 198 by a microtubule disrupter. Mol Pharmacol 2005;68:1415 – 22.

31. Gache V, Louwagie M, Garin J, et al. Identification of proteins binding the native tubulin dimer. Biochem Biophys Res Commun 2005;327:35 – 42.

32. Suh JK, Robertus JD. Role of yeast flavin-containing monooxygenase in maintenance of thiol-disulfide redox potential. Methods Enzymol 2002; 348:113 – 21.

33. Britto PJ, Knipling L, McPhie P, Wolff J. Thiol-disulphide interchange in tubulin: kinetics and the effect on polymerization. Biochem J 2005;389: 549 – 58.

34. Vertessy BG, Bankfalvi D, Kovacs J, et al. Pyruvate kinase as a microtubule destabilizing factor *in vitro*. Biochem Biophys Res Commun 1999;254:430 – 5.

35. Raspaglio G, Filippetti F, Prislei S, et al. Hypoxia induces class III β-tubulin gene expression by HIF-1α binding to its 3′ flanking region. Gene 2008;409:100 – 8.